Transactions of the Materials Research Society of Japan Vol.28 3-6 (2003)

Surface and Interface Roughness Studies by Grazing Incidence X-ray Scattering Method

Shin-ya Matsuno, Zou Fen, Takeshi Nayuki and P. W. T. Yuen*
Analysis and Simulation Center, Asahi KASEI Co. 2-1, Samejima, Fuji, 416-8501, JAPAN
Fax: 81-545-62-3808, e-mail: matsuno.sb@om.asahi-kasei.co.jp
*Winfrith Technology Center, Winfrith, Newburgh, Dorchester, Dorset DT2 8XJ, U.K.
Fax: 44- 0-1305-212103, e-mail: pyuen@qinetiq.com

First, we discussed the validity of two interface roughness models 1) Gaussian and 2) tanh-depth profile for TiN/Si composite. The surface and interface roughness of TiN/Si composite was calculated by using these two models and the result was compared with measured data. The result shows that the tanh-depth profile indicates a better interface roughness model for TiN/Si composite. Second, the surface roughness of SiO_2 thin films on Si wafers were analyzed using a combination of x-ray reflectivity and diffuse scattering methods, and the results were compared with the Atomic Force Microscope (AFM) image. By using a Gaussian roughness model the x-ray scattering analysis shows a good agreement with the AFM data.
Key words: X-ray, Reflectivity, Diffuse Scattering, Surface Roughness, AFM

1. INTRODUCTION

Grazing incidence x-ray techniques have been used extensively for the characterization of surfaces and thin films. Especially x-ray reflectivity measurements have been one of the most powerful structural probes for characterizing morphological properties of thin films in nano-meter scales such as the evaluation of film thickness, density, and interface roughness [1-2]. We have been using these x-ray scattering techniques for more than 8 years to analyse properties of thin films over 3,000 samples within our laboratory [3-4]. In this paper, the application of this x-ray scattering analysis for the surface and interface roughness studies is presented and discussed

2. SAMPLE PREPARATION AND EXPERIMENT

In the first experiment, the TiN film was deposited from a Ti target onto a Si substrate by sputtering and the film was subsequently annealed at 650℃ for 1minute under a nitrogen atmosphere.

In the second study, two samples were made by thermal oxidation of Si(001) wafers. A thick oxide layer was grown on sample 1 by flowing O_2 over the sample at a rate of 8.5 l/min for 2.5 h at 1173 K. For sample 2, the Si wafer was first dipped in etching solution for 2 min and then thermally oxidized at the same temperature and conditions as sample 1 for about 3 hrs.

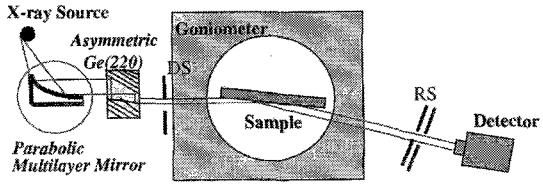

Figure 1. A schematic illustration of the experimental set-up used to measure the x-ray reflectivity and diffuse scattering

The x-ray reflectivity and diffuse scattering measurements were carried out using a x-ray reflectometer (Rigaku ATX-G) as shown in figure 1. X-rays with wavelength λ =1.5405 Å ($CuK_{\alpha 1}$) were generated from a Cu rotating anode (50kV, 300mA) and collimated by a parabolic multilayer mirror and subsequently monochromated by a channel cut Ge(220) asymmetric channel-cut crystal [3-4].

A divergence slit ($0.1 \times 10mm^2$) was utilized to control the exposure area on the sample surface and a couple of receiving slits ($0.2 \times 20mm^2$) were mounted in front of a NaI crystal scintillation counter. Specular reflectivity curves were recorded using $2\theta / \omega$ scans. Diffuse scattering data were taken with 2 theta fixed and to measure ω scans.

3. RESULTS AND DISCUSSIONS

3.1 Evaluation of surface and interface roughness of TiN thin film on Si substrate

The experimental reflectivity curves for the TiN/Si sample are shown in figure 2.

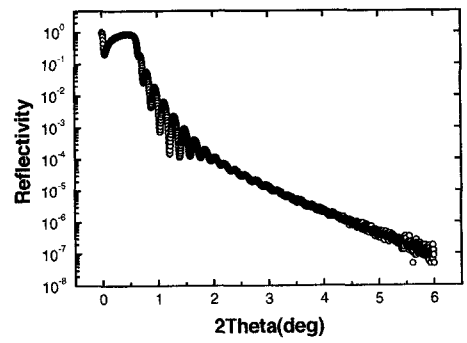

Figure 2. X-ray specular reflectivity curve for TiN film on Si substrate

The experimental data was analyzed by fitting theoretical reflectivity curves derived from Parratt's recursive formula (equations 1 & 2) modified with the distorted wave Born approximation (DWBA). Here, $F_{n-1,n}$ is the Fresnel reflectivity coefficient of the interface between n-1-th layer and n-th layer, d_n the thickness of n-th layer, and $R_{n-1,\,n}$ the reflectivity amplitude of the interface between n-1-th layer [5-7]. Note that a Gaussian profile density function has been implemented in equation (2).

$$R_{n-1,n}=a_{n-1}^{4}\left\{\frac{R_{n,n+1}+F_{n-1,n}}{R_{n,n+1}F_{n-1,n}+1}\right\} \quad (1)$$

$$a_n \equiv \exp\left(-i\frac{\pi}{\lambda}\phi_n d_n\right), R_{n,n+1} \equiv a_n^{2}\frac{E_n^{R}}{E_n}, a_0 \equiv 1$$

$$\phi_n \equiv \left(\theta^2-2\delta_n-i2\beta_n\right)^{\frac{1}{2}}$$

$$F_{n-1,n}' = F_{n-1,n}\exp\left\{-1/2\left(\sigma_{n-1,n}^{2}\frac{16\pi^2}{\lambda^2}\phi_{n-1}\phi_n\right)\right\} \quad (2)$$

The Lenvenvurg-Marquardt method was used to fit the theoretic reflectivity curve with the experimental data (figure 3).

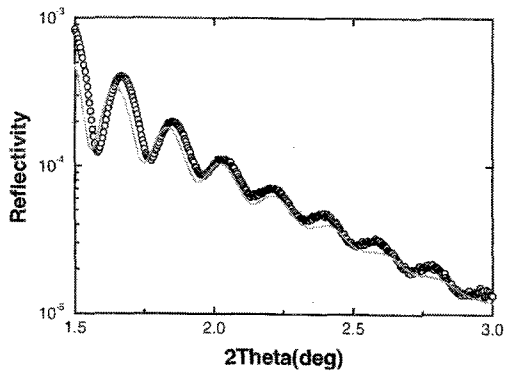

Figure 3. Shows the experimental reflectivity data (open circles) and the fitted theoretical curve (solid line) for TiN film on Si substrate using the Gaussian profile density function.

The fitted result for the parameters of film thickness, surface roughness and interface roughness are found to be 43nm, 2.1nm and 0.4nm, respectively. Although the experimental reflectivity data (open circles) seems to be good resemble to that of the fitted curve (solid line), the thickness fringes of high angle region can not be reproduced in this Gaussian profile model.

Alternatively, another density function using tanh-depth profile can be implemented:

$$P_{\tanh}(z)=\frac{1}{\sqrt{2\pi}\cosh^{2}\left(\sqrt{\frac{2}{\pi z}}/\sigma_{n-1,n}\right)} \quad (3)$$

In fact, the tanh profile is very similar to the Gaussian function used in equation (2) as depicted in figure 4. However, this tanh profile has the advantage that the Helmholtz equation for the electromagnetic fields can be solved analytically, that means without the constraint of $\sigma_{n-1,n}\times k < 1$ which usually is needed in the DWBA [8].

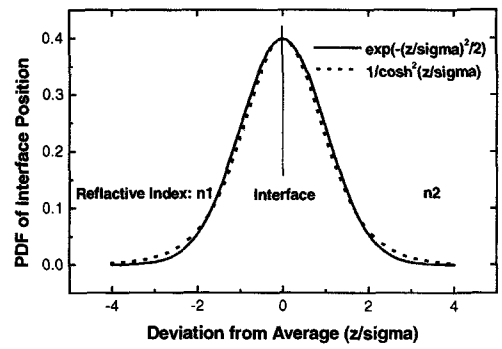

Figure 4. PDF of the Gaussian and tanh profiles roughness models

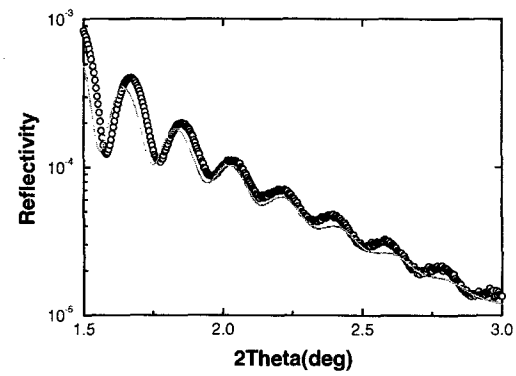

Figure 5. Shows the fitting of the experimental reflectivity data using $P_{\tanh}(z)$ roughness profile.

The experimental reflectivity curve was also analyzed by calculating reflectivity curves using the same parameter (film thickness: 43nm, surface roughness: 2.1nm, interface roughness: 0.4nm) but the model of $P_{\tanh}(z)$. The results are shown in figure 5, and we can see that the fitting patterns are better than Gaussian roughness model. The result shows that the tanh-depth profile indicates a better interface roughness model for TiN/Si composite.

3.2 Simultaneous fitting of the reflectivity curves and the diffuse scans

Reflectivity measurements include some part of the diffuse scattering. This diffuse component is registered, together with the specular beam, by the detector aperture. This contribution can not be neglected at the samples of large-scale roughness. X-ray reflectivity and diffuse

scattering measurements of two kinds of sample of thermal oxidation of Si(001) wafers (as mentioned in section 2: sample preparation) were performed and analyzed simultaneous fitting method [9].

First, the experimental reflectivity curves were analyzed, and film thickness and surface roughness of sample 1 were obtained. The values are 45.6nm and 0.4nm, respectively. For sample 2, weak oscillations of x-ray reflectivity could be observed.

Diffuse scattering data of ω scans (or rocking scans) with 2θ fixed condition are shown in figure 6.

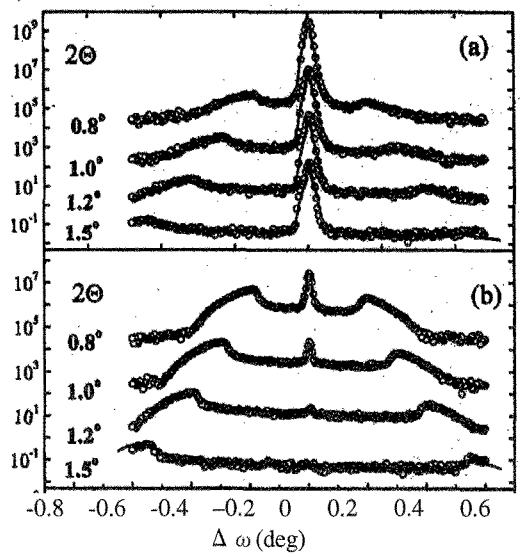

Figure 6. ω scans from sample 1 (a), 2 (b) for offsets 2θ =0.8° , 1.0° , 1.2° , and 1.5°

The ω scan profiles were analyzed simultaneously with the reflectivity data, i.e. the thickness, roughness, and lateral correlation length were calculated to be optimal for the refined fits of both scan types. Here, the correlation function yields to (for self-affine fractal surface) ;

$$C(X_0) = \sigma^2 \exp\left[-\left(\frac{X_0}{\xi}\right)^{2h}\right] \quad (4)$$

where X_0 is the lateral length scale, ξ is defined as the correlation length which is the average length between two points located at the same height in the profile, and h is the Holder coefficient coprised between 0 and 1. Very rough surfaces provide smaller h values while smooth profile gives a h value close to 1, so h is closely related to the fractal dimension D: D=E + 1 – h with E the dimension of the euclidean space; E=1 for a profile; E=2 for a plane.

The obtained results are as follows.

Sample 1:
Thickness of SiO2: 45.6nm (by x-ray reflectivity)
Surface roughness: 0.4nm (by x-ray reflectivity)
Lateral correlation length: ~200nm

Sample 2:
Thickness of SiO2: 65.4nm
Surface roughness: 4.1nm
Lateral correlation length: 10nm

Finally, the AFM studies were carried out for samples 1 and 2 (figure 7(a) and 7(b), respectively). The AFM images confirm the morphology of the surfaces deduced from the x-ray experiments.

4. CONCLUSIONS

In summary, we have shown that model of Gaussian interface roughness was not good approximation on a sample of TiN/Si composite. Tanh-interface roughness model was better approximation than Gaussian model in this case.

We have shown that the combination of x-ray reflectivity and diffuse scattering measurements allows one to characterize the surface morphology of SiO2/Si composite. The AFM imaging results are good agreement with the parameters found from x-ray technique.

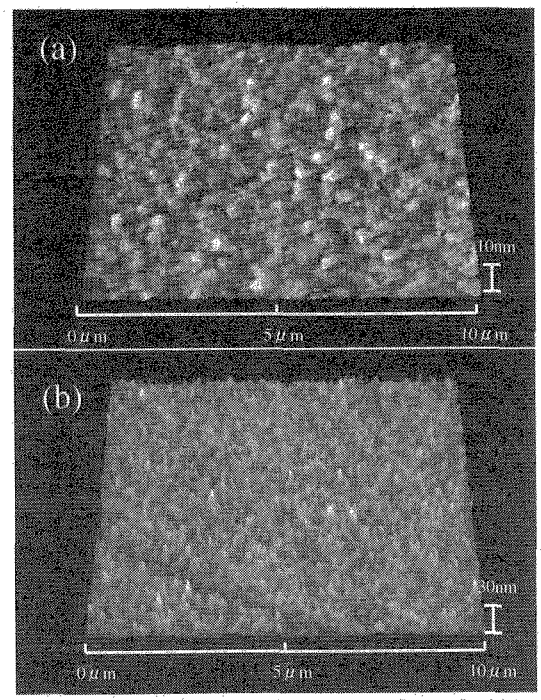

Figure 7. AFM images of the surface of sample 1(a) and 2(b). Sample 2 exhibits large-scale roughness (in other words, very jagged surface) similar to an island-like morphology.

Acknowledgment

We are grateful to the heads of Analysis and Simulation Center; Mr. Susumu Tanji, Mr. Kenji Kanekiyo, and Dr. Hideaki Imai for their support and encouragement. Also we would like to thank all the members of our section for their interest to this study.

References

[1] D.K. Bowen and M. Wormington, *Adv. X-Ray Anal.*, **36**,171 (1993)
[2] T.C. Huang, *Adv. X-Ray Anal.*, **38**, 139 (1995)

[3] Shin-ya matsuno, Masayuki Kuba, Takeshi Nayuki, Suketaka Soga, and P. W. T. Yuen, *The Rigaku Journal*, VOL **17**, No.2 36 (2000)
[4] Shin-ya Matsuno, Masayuki Kuba, Yoshitaka Moriyasu, Takashi Morishita, and Kazuhiko Omote, *Adv. X-Ray Anal.*, **43**, 177 (2000)
[5] L. G. Parratt, *Phys. Rev.* **95**, 359 (1954)
[6] P. Croce and L. Nexot, *Rev. Phys. Appl.*, **11**, 113 (1976)
[7] K. Sinha, E. B. Sirota, S. Garoff, and H. B. Stanley, *Phys. Rev.* **B 38**, 2297 (1988)
[8] D. Bahr, W. Press, R. Jebasinski, and S. Mantl, *Phys. Rev.* **B 47**, 4385 (1993)
[9] A. Ulyanenkov, K. Omote, R. Matsuo, J. Harasa, and S. –Y. Matsuno, *J. Phys. D: Appl. Phys.* **32**, 1313 (1999)

(Received July 21, 2003; Accepted August 21, 2003)